NOVEL METHOD FOR PHASE-SPACE TOMOGRAPHY OF RAPIDLY EVOLVING E-BEAMS

K. Chalut, Duke University, Department of Physics, Durham, NC 27708, U.S.A,
V.N. Litvinenko, I.V. Pinayev, Brookhaven National Laboratory, Upton, NY 11973, U.S.A.

Abstract

In this paper, we describe a new method for phase-space tomography. This method allows one to restore phase space density using a small number of projections covering a limited angle of rotation or another linear transformation in the phase space. Practical applications of this method for phase-space tomography are discussed.

INTRODUCTION

Traditional methods of phase-space tomography, such as the Radon transform, require multiple, evenly spaced projections of exactly a 180° rotation angle in the phase-space in order to reconstruct a frozen picture [1]. It means that reconstruction of the longitudinal phase space of the e-beam with Radon transforms require the evolution of the e-beam to be slow (adiabatic) on the time scale of synchrotron oscillations. Radon transforms also apply only to rotations, i.e. to a very small sub-group of linear transformations and projections used in accelerator physics and, generally, in imaging.

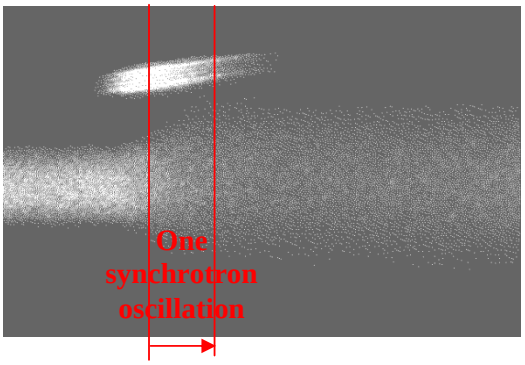

Figure 1: Dual-sweep streak camera image of giant pulse. The camera recorded the time structure of the intensity of the light generated by the e-beam on multiple turns. The vertical sweep, which is synchronized with the revolution of the e-beam, is fast and has the full scale of 1.6 nsec. The horizontal sweep is slow and has the full scale of 500 μsec. The trace seen at top is the FEL light. The main image is that of the spontaneous radiation of electron beam, which is identical to the beam time profile.

In the giant pulse process in a storage ring FEL [2], the electron beam evolves dramatically and its energy spread increases by up to a factor of three within one synchrotron oscillation. For the giant pulse process, and other processes that evolve quickly, a new method of reconstruction is needed. We investigate two new methods of reconstruction that are not limited by observation angle, and work for any linear process, not just rotation. The only requirement is that we have some known set of linear projections.

METHOD DESCRIPTION

Projection matrix

Suppose we have an arbitrary distribution of particles $F(\vec{X}_n,\vec{P}_n)$ in an N^D phase space (*D* is its dimension), described by its spatial $(\vec{X})$ and momentum $(\vec{P})$ coordinates, it follows that there is a projection operator $\hat{P}(\alpha)$ which, when acting upon the distribution, will give us a set of linear projections (images) $I(\vec{x}_m,\alpha)$ where

$$I(\vec{x}_m,\alpha)=\hat{P}(\alpha)\otimes F(\vec{X}_n,\vec{P}_n). \qquad (1)$$

$\vec{x}_m$ is the sub-set of spatial coordinates in the projection (image) space. Typical projection space used for imaging beam of charged particles has one or two dimensions. The projection matrix depends only upon the parameter α, which we use to identify projection.

In our specific example we used a dual sweep streak camera (hence one dimensional images) for reconstruction of an evolution of electron beam density (*F*) in longitudinal phase space (two dimensions). But the method is applicable of any process with linear transformations and projections [3].

The longitudinal phase space of electron beam in a storage ring can described by two dimensionless coordinates $\varepsilon=(E-E_0)/\sigma_{E0}$ and $\zeta=(t-t_0)/\sigma_{t0}$, where *E* and *t* are the energy and arrival time of an electron, E_o and t_o are, respectively, the energy and time of the synchronous electron, σ_{E0} and σ_{t0} are corresponding RMS spreads of a stationary beam. Electron bunches under study are very short and the unperturbed motions of electrons in the longitudinal phase space can be presented as a simple rotation in which the angle is the synchrotron phase advance φ:

$$\begin{bmatrix}\varepsilon\\ \zeta\end{bmatrix}_n=\begin{bmatrix}\cos\varphi_n & \sin\varphi_n\\ -\sin\varphi_n & \cos\varphi_n\end{bmatrix}\cdot\begin{bmatrix}\varepsilon\\ \zeta\end{bmatrix}_o;\varphi_n=n\cdot 2\pi Q_s \quad (2)$$

where $Q_s << 1$ is synchrotron tune [4] and *n* is the turn number. The rotation causes a transformation of the phase space density governed by the Liouville theorem:

$$F_n(\zeta,\varepsilon)=F_0(\zeta\cdot\cos\varphi_n-\varepsilon\cdot\sin\varphi_n,\varepsilon\cdot\cos\varphi_n+\zeta\cdot\sin\varphi_n) \quad (3)$$

At each turn of the e-beam around the ring the dual sweep streak camera records the time profile of the beam, i.e. the projection of the phase space density F(E,ζ) onto the time coordinate:

$$I(\zeta\cdot\sigma_{to})_{\varphi}=P(\varphi)\otimes F_o(\zeta,\varepsilon)=\int_{-\infty}^{\infty}F(t/\sigma_{to},\varepsilon)\cdot d\varepsilon= \int_{-\infty}^{\infty}F_o(\zeta\cdot\cos\varphi_n-\varepsilon\cdot\sin\varphi_n,\varepsilon\cdot\cos\varphi_n+\zeta\cdot\sin\varphi_n)\cdot d\varepsilon \quad (4)$$

Hence in our case the projection operator is completely defined by the synchrotron phase φ. This is still a description using continuous functions and coordinates. To make the problem computer friendly we must translate this problem into arrays and bits of information. Let's consider that we have a distribution function defined on an *N x N* grid in the phase space, $F=[F_{ij}]$. Our goal is now to find a way to extract information about the array F from the finite number of projections.

We get our full set of linear projections from a dual-sweep streak camera [5], which captures the synchrotron light from the electrons. A CCD camera digitizes the images from the streak camera. Let's select a sub-set of *J* projections (along vertical lines in Fig. 1), which cover a small portion of a synchrotron period, and use *M* pixels from each image. The information contained in these projections has $J \times M$ bits. As long as $J \times M > N^2$ we have a chance to extract the information about the distribution function $F=[f_{ij}]$.

The matrix form of equation (1) takes following form:

$$[I]_u=[P]_{u,v}\cdot[F]_v;\quad u=N^{2D};v=M\cdot J \quad (5)$$

where array *I* is a combination of ordered J projections, *F* is the array of ordered F_{ij}, and ***P*** is the projection matrix, specific appearance of which we define later. In the case of the giant pulse process in a storage ring FEL, the relevant parameter for the projection matrix is the synchrotron phase, and knowing the synchrotron frequency and the time of each projection provides us with that knowledge.

The problem is now reduced to a robust way of solving equation (1) and finding F with reasonable accuracy. The projection matrices are typically very large, non-square and singular, which makes singular value decomposition (SVD) method a natural choice for solving equation (1).

SVD

There is a wealth of information concerning SVD (see for instance [6]), but it is, in brief, the decomposition which, when inverted, satisfies the least-squares minimum criteria for the function

$$\Phi=\left\|I-P\cdot F\right\|^2 \quad (6)$$

One decomposes a matrix $P\rightarrow UDV^T$, where the columns of U are the eigenvectors of PP^T, the columns of V are the eigenvectors of P^TP, and D is a diagonal matrix comprising the singular values (square root of the eigenvalues) of PP^T. U and V are, by definition, orthogonal. This decomposition can be inverted (pseudoinverse) as $P^+=VD^+U^T$, where the diagonal of D^+ is made up of the inverse of each of the singular values of D, in descending order, so long as the singular value in question is not zero. If the singular value of D is zero, then the corresponding element of D^+ is also zero. If we assume ***P*** is a $u\times v$ matrix, then as *u* increases, some diagonal elements of D^+ can be very large, and undue emphasis can be put on the corresponding singular values. This may cause a very high sensitivity of the method to errors and noise. Fortunately, SVD allows us to truncate the series at any desirable number of eigen values (which are all positive, or zero, and are numerated in descending order) with any $K \le min\ (u,v)$:

$$P^+=\sigma_1E_1+\ldots\sigma_KE_K=\sum_{k=1}^{K}\sigma_kE_k;\ E_k=\left|U_k\right\rangle\left\langle V_k\right|. \quad (7)$$

Truncation provides for robustness of this method and makes it less sensitive to the errors in the knowledge of projection matrix as well as to the noise in the images. The projection matrix is defined both by the type of projection (for example the angle of rotation), the size of the pixel in the image array and the type of discrete representation of a continuous distribution. Here we present two simple discrete models representation: pillbox and Gaussian.

Pillbox representation

This is a simple representation of the distribution by *NxN* pillboxes with F_{ij} height located on an evenly spaced 2D-grid.

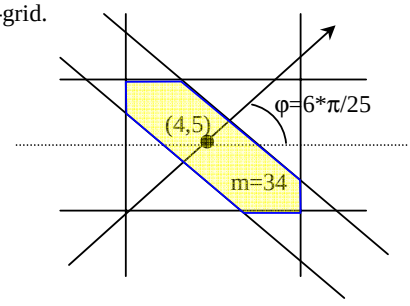

Figure 2: Element of projection matrix $P_{634,31}$ of grid-box (4,5) on the 34th pixel when the grid is rotated on the angle of φ =6*π/25 around the origin is equal to the area of the intersection shaded in light yellow.

The elements of the projection matrix are equal to the area of intersection of a box located on (i,j)-grid node with the lines indicating the boundaries of the m[th] pixel. The grid rotates around the origin according to the angle φ of given projection. Figure 2 shows a specific example of such a cross-section:

$$P_{m,j,i,l}=P_{634,35}=Area_{ovelap} \quad (8)$$

The pillbox representation has the advantage of giving the exact projection matrix, but the sharp corners inherent in the method do not provide for a smooth reconstruction. Hence, these sharp corners can be exaggerated in the presence of errors or/and noise.

Gaussian representation

It is a more elegant representation of a distributed function by a set of *NxN* Gaussians centered at the evenly spaced 2d-grid - see equation (9a). Each Gaussian has individual height (F_{ij} for (i,j)th node) and a common r.m.s. width σ_r, which plays the role of an adjustable parameter.

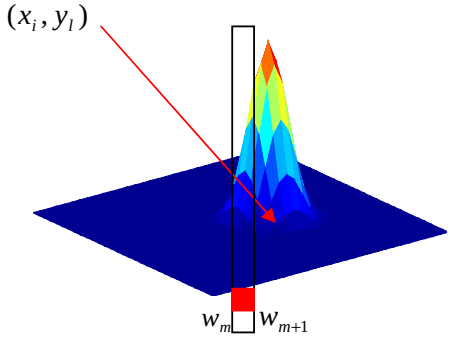

Figure 3: The projection of a pixel onto a Gaussian node in the phase-space.

The projection matrix is then found by projecting each Gaussian mode onto each pixel using eq. (4) and the pixel width (w_m,w_{m+1}):

$$(a)\ F(x,y)=\sum_{i,l}F_{i,l}*e^{-\frac{1}{2\sigma_r^2}(-(x-x_i)^2-(y-y_l)^2)}$$
$$(b)\ P_{m,i,j,l}=\sqrt{2\pi}\sigma_{rep}\int_{w_m}^{w_{m+1}}e^{-\frac{1}{2\sigma_r^2}(x_i\cos\varphi_j+y_l\sin\varphi_j-u)}du \qquad (9)$$

Solution

When projection matrix is pseudo-inverted for a given choice of K (i.e. cut-off number of eigen vectors used in reconstruction) using eq. (7), the $P^+(K)$ gives the resulting elements of F_{il} as:

$$[F]=[P^+(K)]\cdot[I]. \qquad (7')$$

In pillbox case these are the heights of the boxes on the grid with discontinuities on each grid edge. For Gaussian representation, the result is a smooth function (9a), whose scale of variations can be limited by increasing of σ_r. Increase of σ_r to or above a size of a grid size will also lead to the reduction of the accuracy of the representation. Hence, there is an optimum σ_r (depending of the errors and the noise level), which provides a smooth but reasonable accurate representation of the real distribution function.

THEORETICAL COMPARISON

In order to study the theoretical aspects of the two representations, we created a theoretical construction, wherein we may compare a known function with our reconstruction. Here we present few selected results with the trial function a Gaussian with unit height, located off-origin and having r.m.s. width of 2 grid size. Both representations were using 13x13 2D-drid with using grid size. Theoretical projections are 117 pixels for each image (an arbitrary number). We then use the SVD method described above for both representations. We evaluated the accuracy of reconstruction by subtracting the theoretical numbers from the reconstruction on the grid and comparing the norm of the difference with the norm of original function:

$$Error[\%]=\frac{norm(reconstruction-baseline)}{norm(baseline)}*100$$

Figure 4 shows results of preliminary studies of the methods accuracy as function of the number of projections (spaced 10° apart).

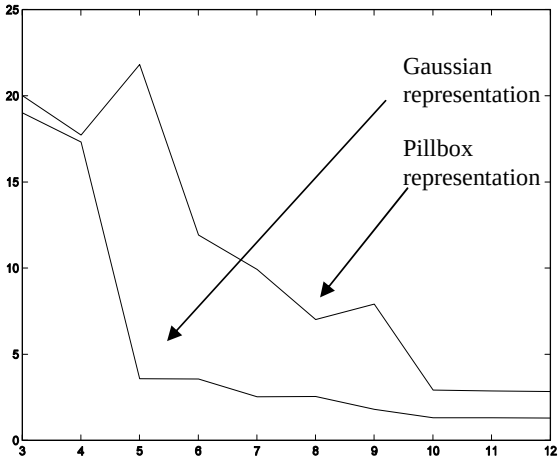

Figure 4: Error of reconstruction vs. # projections for pillbox and Gaussian representations.

We did not succeed so far in accurate reconstructing of the trial functions using two projections and limited number of pixels ~ 100 - the errors are too large. We attribute it either to a need for a better image resolution (M >> 100) or to a possible "small bugs" in our programs. It is clear from our preliminary studies that the Gaussian representation provides a better reconstruction for smooth functions than the pillbox representation. We continue the studies of the analytical features of the method, including reconstruction of distributions with complex topology.

ANALYSIS OF GIANT PULSES

Figure 1 shows one of many measured dual sweep streak camera images of electron beam evolution in the Duke OK-4 storage ring FEL during the giant pulse process. During the above measurement the synchrotron frequency was 24.3 kHz, and the image shows evolution of the longitudinal distribution of the electron beam over

approximately 12 synchrotron oscillations. One can see that there is a transition region, where the length if the e-bunch is evolving rapidly, and dramatically, in less than one synchrotron oscillation.

The self-consistent theory of giant pulses [7] predicts strongly asymmetric, snail-like distribution [8] generated in the giant pulse process. Out new method allows us to reconstruct distributions from a limited number of projections, to observe the details of phase space dynamics during the giant pulse and to compare them with the theory. Preliminary results look promising, as seen in the pictures below.

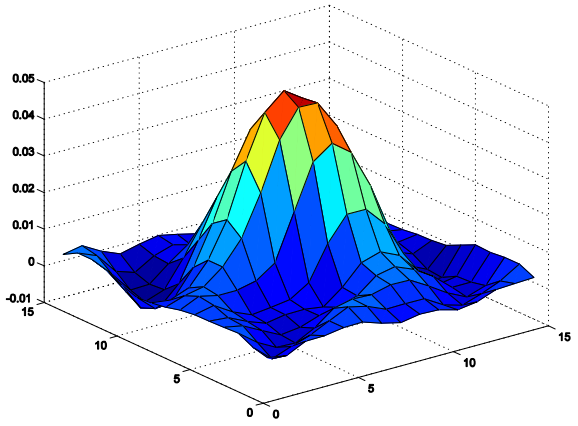

Figure 5: Reconstruction of e-beam distribution in equilibrium (before lasing) using 8 projections, 6.82° apart. Scale is arbitrary.

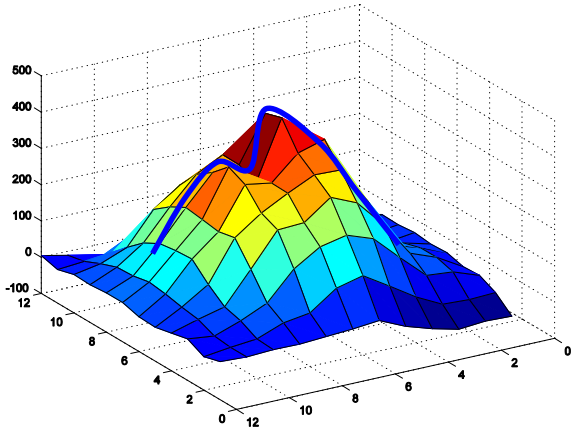

Figure 6: A reconstruction using 8 projections, 6.81° apart, of the transition region. Noticeable double-hump is remarkably similar to the profile predicted by the theory [7,8].

The pictures in Figures 5 and 6 were reconstructed using the Gaussian representation. The reconstructions using the pillbox representation had many jagged peaks.

The reconstructed distribution shown in Fig. 6 qualitatively agrees with the theoretical prediction [7,8]. Clearly, there is room for more studies and comparisons. We plan to finish detailed comparison of a giant-pulse simulation using #vuvfel code [8] (with beam parameters taken from experimental runs) and to compare the simulated electron distributions with the reconstructions we get from dual-sweep streak camera images. The reconstruction passes the eye test, but the next step is to do a quantitative comparison. We stress that only 8 projections, space 6.82° apart, were used to complete this reconstruction, for a total observation angle of 47.8°. There is reason to believe some improvements can be made on the code so that we can get a better reconstruction with an even smaller set of projections.

CONCLUSIONS

We developed a novel method of phase-space tomography, which theoretically requires only a full set of two or more linear projections. Currently, we are improving the model to see how low the limit can be pushed. Theoretical models indicate that, with limited resolution, we can get a good reconstruction (<5%) with a set of five projections. Perhaps we could get better reconstruction using greater resolution. We used experimental data from giant-pulse measurements at the Duke storage ring FEL to test the model, and saw some promising results.

It is important that this method works for any linear projections, not only for rotations [3]. It has potential applications of this method for accelerator physics, medicine, military, and astronomy. Future work will be to further improve the model, compare it to giant-pulse simulations, and apply the method to other problems.

REFERENCES

[1] S.R. Deans, The Radon Transform and Some of Its Applications, Wiley & Sons, 1983.

[2] I.V. Pinayev et al., Nucl. Instr. and Meth. A475 (2001), pp. 222-228

[3] SVD-based tomography, K.Chalut, V.N. Litivinenko. in preparation

[4] see for example, “The Principles of circular Accelerators and Storage Rings”, Philip J.Briant and Kjell Johnsen, Cambridge University Press, 1993, p.156

[5] A.H. Lumpkin et al., Nucl. Instr. and Meth. A407 (1998), pp. 338-342.

[6] P.E.Gill et al, Numerical Linear Algebra and Its Optimization, Addison-Wesley, 1989.

[7] V.N. Litvinenko, Proceedings of FEL conference, August 2002, APS, Argonne, IL, Eds. K.-J.Kim, S.V.Milton, E.Gluskin, p. II-1

[8] V.N. Litvinenko et al., Nucl. Instr. and Meth. A358 (1995), pp. 334